Biological productivity, terrigenous influence and noncrustal elements supply to the Central Indian Ocean Basin: Paleoceanography during the past ∼ 1 Ma

J N Pattan[1*], Toshiyuki Masuzawa[2], D V Borole[1], G Parthiban[1], Pratima Jauhari[1] and Mineko Yamamoto[3]

[1] *National Institute of Oceanography, Dona Paula, Goa 403 004, India.*
[2] *Department of Hydrospheric–Atmospheric Sciences, Graduate School of Environmental Studies, Nagoya University, Nagoya 464-8601, Japan.*
[3] *Hydrospheric–Atmospheric Research Centre, Nagoya University, Nagoya 468-601, Japan.*
[*] *e-mail: pattan@darya.nio.org*

A 2 m-long sediment core from the siliceous ooze domain in the Central Indian Ocean Basin (CIOB; 13°03′S: 74°44′E; water depth 5099 m) is studied for calcium carbonate, total organic carbon, total nitrogen, biogenic opal, major and few trace elements (Al, Ti, Fe, K, Mg, Zr, Sc,V, Mn, Cu, Ni, Zn, Co, and Ba) to understand the productivity and intensity of terrigenous supply. The age model of the sediment core is based on U–Th dating, occurrence of Youngest Toba Tuff of ∼ 74 ka and Australasian microtektites of ∼ 770 ka.

Low carbonate content (< 1%) of sediment core indicates deposition below the carbonate compensation depth. Organic carbon content is also very low, almost uniform (mean 0.2 wt%) and is of marine origin. This suggests a well-oxygenated bottom water environment during the past ∼ 1100 ka. Our data suggest that during ∼ 1100 ka and ∼ 400 ka siliceous productivity was lower, complimented by higher supply of terrigenous material mostly derived from the metasedimentary rocks of High Himalayan crystalline. However, during the last ∼ 400 ka, siliceous productivity increased with substantial reduction in the terrigenous sediment supply. The results suggest that intensity of Himalayan weathering, erosion associated with monsoons was comparatively higher prior to 400 ka. Manganese, Ba, Cu, Ni, Zn, and Co have around 90% of their supply from noncrustal (excess) source and their burial to seafloor remained unaffected throughout the past ∼ 1100 ka.

1. Introduction

Changes in the chemical composition of source material, bioturbation and diagenesis are the main factors controlling the variation in the composition of bulk sediment with time and are related to climate change (Fenney *et al* 1998). The sediments and their variation through time therefore, record the erosion and uplift history of that region (Cochran 1990). Due to the uplift and erosion of Himalayas, an enormous volume of sediment reached the Bengal fan and subsequently the Central Indian Ocean Basin (CIOB) via the Ganges and the Bramhaputra river system. The abundance of this terrigenous material decreased towards the south (Aoki *et al* 1973; Nath *et al* 1989; Bouquillon *et al* 1990; Cochran 1990; Debrabant *et al* 1993; France-Lanord and Derry 1993; Fagel *et al* 1994; Derry and France-Lanord 1996). Studies on the ODP Leg 116 south of Equator (1°S; 81°24′E) demonstrated that the sediments during lower Miocene to upper Miocene were derived mostly from Himalayas, from Upper Miocene to Middle Pleistocene sediments were derived from

Keywords. Calcium carbonate; organic carbon; biogenic opal; detrital elements; sediment; Central Indian Ocean Basin.

© Printed in India.

the Indian subcontinent (Bouquillon *et al* 1990; Brass and Raman 1990) whereas, during Middle Pleistocene to Holocene period sediment input from the Himalayas resumed again.

Based on the chemical and isotopic studies of clay minerals, France-Lanord and Derry (1993); Derry and France-Lanord (1996) suggested that irrespective of clay mineral variations, the sediments were derived only from the Himalayas and that the change in clay minerals are due to different degrees of weathering. It has been reported that the northern part of CIOB receives detrital material derived from the denudation of Himalayas (Kolla and Biscaye 1973; Nath *et al* 1989; Debrabant *et al* 1993; Fagel *et al* 1994) whereas, the southern part receives siliceous pelagic input associated with equatorial divergence at 10°S (Pattan *et al* 1992; Caulet 1992; Banakar *et al* 1998). In CIOB, a few short sediment cores covering a time span of less than 200 ka have been studied earlier mostly for transition metals (Banakar *et al* 1991; Mudholkar *et al* 1993; Borole 1993a and b) but a detailed study on productivity proxies, major and trace element geochemistry for a longer time span is lacking. In the present study, we have analysed calcium carbonate, total organic carbon, total nitrogen, biogenic opal, major and few trace elements to understand the productivity, and variation in terrigenous material supply to the CIOB during the last $\sim$ 1100 ka.

2. Materials and analytical methods

A 2 m-long gravity sediment core (AAS-05/GC-02) from a siliceous ooze domain of the CIOB (13°03′S: 74°44′E; water depth of 5099 m) collected during the 5th expedition of *A A Sidorenko* in 1994 under a Polymetallic Nodule programme has been studied here (figure 1). The sediment core was subsampled on board at 2-cm interval from core top up to 150 cm and at 5-cm interval from 150 to 200 cm. During sub-sampling, a dispersed ash layer was noticed between 30 and 40 cm depth and a few buried nodules at the core top. The dried and powdered sediments were subjected to the following investigations.

2.1 *Uranium–Thorium dating*

About 2 to 3 g of bulk sediment was digested in a Teflon beaker with HF, $HClO_4$ and HCl in the presence of $^{232}U/^{228}Th$ spike. Uranium–Thorium radiochemical separation and purification were carried out following the standard procedure of Krishnaswami and Sarin (1976). The alpha activity of the electroplated sample was assayed using ion implanted detector coupled to Octete plus Alpha spectrometer (EG & G - Ortec).

2.2 *Electron microprobe analysis and scanning electron microscopy*

Volcanic glass shards from the coarse fraction ($> 63\,\mu$m) were cleaned ultrasonically, mounted in an epoxy resin, polished to expose the internal features and analysed for major elements on an Electron Probe Micro Analyser (Cameca SX-50). Morphology of glass shards was studied under a Scanning Electron Microscope (JSM-5800LV).

2.3 *Microtektites*

From the coarse fraction, > 125 size fraction was separated and examined for the occurrence and abundance of microtektite under a binocular microscope. The Australasian microtektites have an age of $\sim$ 770 ka and their abundance in the core depth reflects a sediment accumulation rate.

2.4 *Total organic carbon, total nitrogen and calcium carbonate*

The bulk sediment was decarbonated initially by treating overnight with 1M HCl followed by 0.1 M HCl and later by milli-Q water. Organic carbon (C_{org}) and total nitrogen (N_{tot}) content were measured with a Carlo Elba NA-2500 elemental analyser. The instrument was calibrated for carbon (peak area) and nitrogen (peak height) by using Acetelinide standard along with a blank. The slope and intercept of carbon and nitrogen remained almost constant during daily calibration. Duplicate analysis of samples showed a precision better than 3%. Total carbon was measured on the bulk sediment following the procedure similar to C_{org}. From total carbon, organic carbon was subtracted to get the inorganic carbon.

2.5 *Biogenic opal*

Biogenic opal was extracted from the bulk sediment by using 2 M Na_2CO_3 at 85°C for 5 hours following the procedure of Mortlock and Froelich (1989). The reference standard material (OF-I) was used to check the accuracy of the data and was found better than $\pm 4\%$. The precision of the data based on duplicate analyses was within the acceptable limit.

2.6 *Major and trace elements*

For the major and trace element analysis, the sediment was treated with an acid mixture of HNO_3, $HClO_4$ and HF in a PTFE vial in a microwave. After digestion the solution was evaporated to near dryness under an infra-red lamp on a hot plate in a draft chamber. The residue was brought into

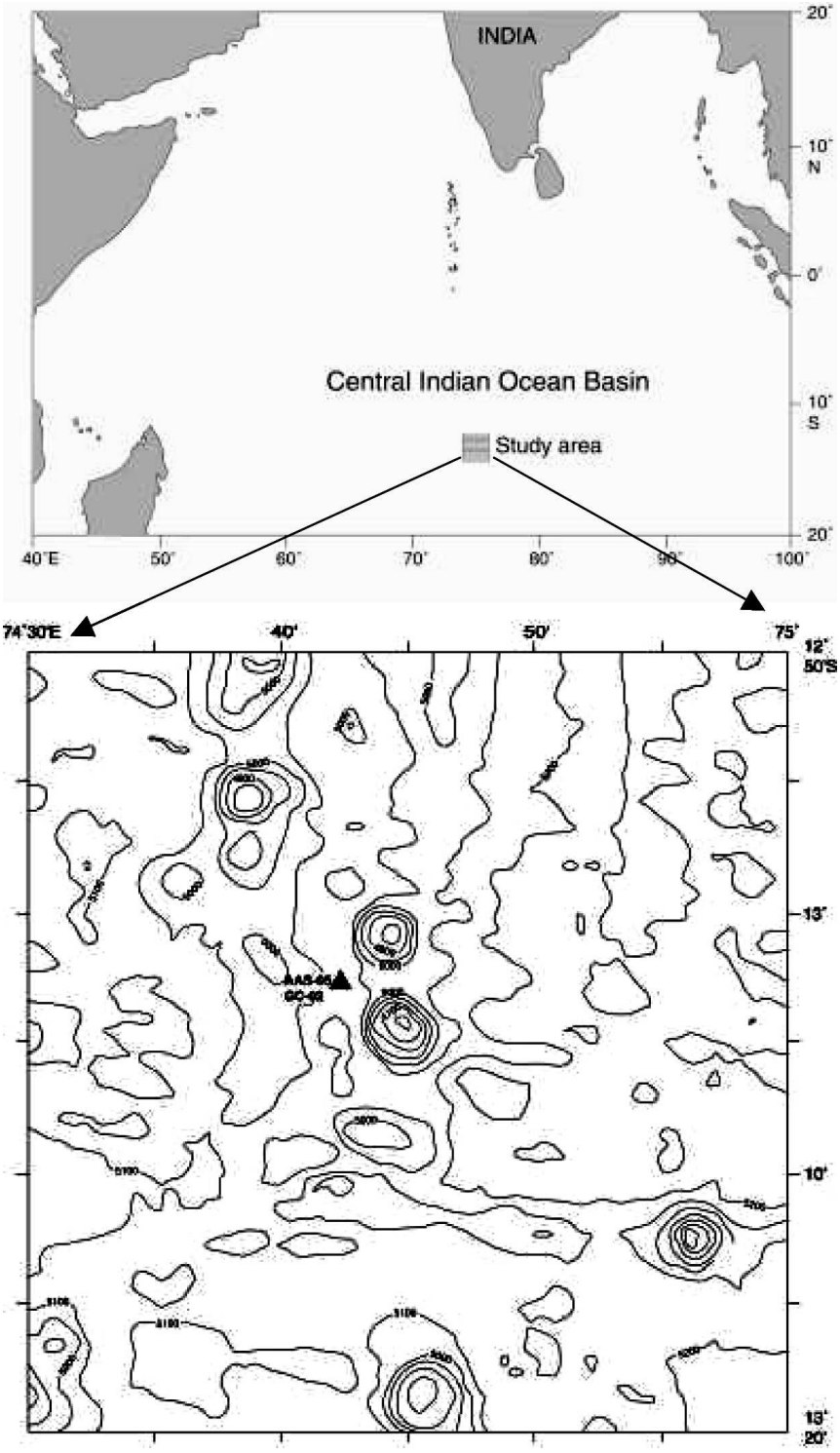

Figure 1. Location map showing study area (top) and the sediment core location (AAS-05, GC-02) with detailed bathymetry (bottom).

clear solution with 2 M HNO_3 and the final volume was made. These samples were analysed for major and few trace elements with a Thermos Jarrel Ash IRIS-AP on inductively coupled plasma–atomic emission spectrometry. An international reference standard material (JB-2) supplied by Geological Survey of Japan (Imai *et al* 1995) was used to check the accuracy that was better than ±5% for the elements and precision of the analyses was within the acceptable limit.

2.7 *Elemental excess or noncrustal source*

Elemental excess or noncrustal source of elements were calculated using the following relation

$$\mathrm{Elem_{excess}} = \mathrm{Elem_{tot}} - (\mathrm{Ti_{sample}} \times \mathrm{Elem/Ti_{GB}}).$$

In the above calculation, we have used Ganges–Brahmaputra particulate (GB) matter data and PAAS data is used wherever GB data is not available. Element excess is expressed in % compared to its bulk concentration.

3. Results and discussion

3.1 *Age model*

The age model for the sediment core is based on Uranium–Thorium dating, presence of Youngest Toba Tuff of ∼ 74 ka and Australasian microtektites event of ∼ 770 ka.

3.1a *Uranium–Thorium dating*

The radiochemical data are presented in table 1. The excess ^{230}Th (^{230}Th: portion of the ^{230}Th that is not supported by the decay of ^{234}U in the sediments) was calculated by subtracting the ^{234}U from the total ^{230}Th activity. The $^{230}\mathrm{Th_{exc}}$ is obtained from the following equation

$$^{230}\mathrm{Th_{exc}}(\mathrm{dpm/g}) = ^{230}\mathrm{Th}(\mathrm{dpm/g}) - ^{234}\mathrm{U}(\mathrm{dpm/g}).$$

The $^{230}\mathrm{Th_{exc}}$ decay profile is shown in figure 2. From 0 to 85 cm the core yields a sedimentation rate of 4.5 ± 0.14 mm/ka ($n = 7$, $r = -0.99$ and $p \leq 0.001$) whereas from 85 to 150 cm core depth yields a sedimentation rate of 2.05 ± 0.09 mm/ka ($n = 6$, $r = -0.99$, and $p \leq 0.001$). The error on the age is derived from the error on the slope for log-linear plot of depth *vs.* ^{230}Th excess for both the fits. Thus, the uncertainty involved in the age–depth model is 3.2% for the top 0–85 cm and 4.5% for 85 to 150 cm depth. These sedimentation rates have been used for calculating the age model of the sediment core. The sediment accumulation rates of 4.5 mm/ka and 2.03 mm/ka are within the range as previously reported (Banakar *et al* 1991; Borole 1993b).

Table 1. *Results of uranium–thorium isotopes in the sediment core.*

Core depth (cm)	^{234}U (dpm/g)	^{230}Th (dpm/g)	$^{230}\mathrm{Th_{exc}}$ (dpm/g)
0–2	0.71 ± 0.52	83.4 ± 3.5	82.7 ± 3.54
12–14	1.26 ± 0.9	70.7 ± 2.33	69.42 ± 2.5
28–30	1.18 ± 0.10	50.6 ± 1.82	49.01 ± 1.82
42–46	0.52 ± 0.18	36.6 ± 1.63	36.10 ± 1.64
56–58	0.52 ± 0.12	29.2 ± 1.84	28.66 ± 1.84
70–72	0.68 ± 0.06	22.0 ± 0.81	21.35 ± 0.81
84–86	0.74 ± 0.13	15.3 ± 0.63	14.53 ± 0.64
100–102	0.74 ± 0.13	7.97 ± 0.44	7.21 ± 0.46
114–116	0.74 ± 0.13	4.98 ± 0.23	4.24 ± 0.26
130–132	0.64 ± 0.06	2.14 ± 0.13	1.5 ± 0.14
142–144	0.54 ± 0.08	1.98 ± 0.18	1.44 ± 0.2
148–150	0.60 ± 0.08	1.30 ± 0.03	0.69 ± 0.08

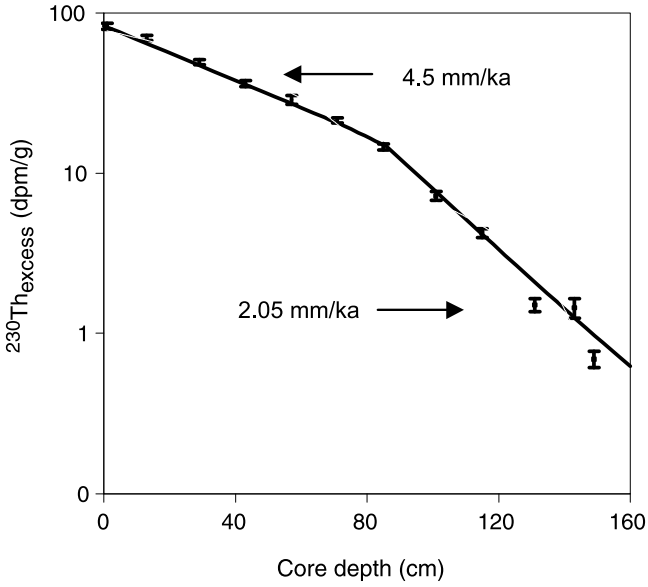

Figure 2. $^{230}\mathrm{Th_{exc}}$ concentration as a function of depth in a sediment core.

3.1b *Ash layer*

Coarse fraction ($> 63\,\mu$m) of the sediment core contains dispersed glass shards at the core top. They become abundant between 30 and 40 cm depth and reach a maximum concentration at 36 and 38 cm. Glass shards appear to be fresh with different sizes, shapes and luster. They are colourless, isotropic and exhibit no signs of alteration. A majority of glass shards are bubble wall junction type (flat/cuspate). Pumice shards have cellular and elongated parallel vesicles. The bubble wall morphology and absence of any blocky or pyramidal morphology suggests a magmatic type of origin. The glass shards have high silica (77 wt%) and total alkali content (6.6 wt%) suggest a rhyolitic composition. They contain low FeO (0.86 wt%), CaO (0.79 wt%), TiO_2 (0.055 wt%). MgO (0.044 wt%) and MnO (0.09 wt%) (table 2). In general, the chemical composition of glass is similar to the Youngest Toba Tuff from Toba caldera of northern Sumatra (∼ 74 ka) and as reported earlier from the CIOB (Pattan *et al* 1999 and references therein). The lower Na_2O values in these glasses may be due to volatilization under the electron beam, which correspondingly results in higher SiO_2 (Shane *et al* 1995). The maximum abundance of glass shards at 36 and 38 cm depth in the sediment core suggests

Table 2. *Electron microprobe data of glass shards from a sediment core in the Central Indian Ocean Basin.*

Oxides	1	2	3
SiO_2	78.70 (0.29)	76.81 (0.22)	77.58 (0.23)
Al_2O_3	12.38 (0.25)	12.77 (0.12)	12.60 (0.13)
TiO_2	0.055 (0.02)	0.07 (0.04)	0.06 (0.04)
FeO	0.86 (0.05)	0.92 (0.07)	0.90 (0.05)
MnO	0.09 (0.05)	0.06 (0.04)	0.06 (0.03)
MgO	0.044 (0.07)	0.05 (0.03)	0.05 (0.02)
CaO	0.79 (0.06)	0.79 (0.07)	0.77 (0.07)
Na_2O	2.07 (0.29)	3.41 (0.13)	3.24 (0.13)
K_2O	4.61 (0.07)	5.08 (0.16)	4.96 (0.14)
Cr_2O_3	0.038 (0.02)	NA	NA
H_2O	3.83 (0.85)	5.23 (0.16)	1.99 (0.83)
N	5	91	275

Recalculated on water free basis. NA = not analysed. (**1**) = present study. (**2**) = Pattan *et al* 1999. (**3**) = Westgate *et al* 1998.

a sediment accumulation rate of 4.8 mm/ka which compliments the sediment accumulation rate of 4.5 mm/ka obtained by U–Th technique for the top 0–85 cm of the core.

3.1c *Microtektites*

The Australasian tektite strewn field is the youngest of the four known fields, its ejecta being distributed over 50 million km^2 that encompasses most of the Indian Ocean. The present sediment core is well within the geographic limits of the Australasian tektite strewn field. This strewn field has an age of $\sim$ 770 ka (Kunz *et al* 1995) and microtektites belonging to this field have been found at over 50 locations (Glass and Wu 1993; Prasad and Khedekar 2003). Microtektites belonging to the Australasian tektite strewn field were searched in this core in the size fraction of $> 125\,\mu$m. The highest peak of microtektite abundance was found at 170 cm depth in the core (Shyam Prasad 2004, unpublished data) which corresponds to an age of $\sim$ 770 ka and provides a sedimentation rate of $\sim$ 0.8 mm/ka between 150 cm and 170 cm depth of the core.

To summarize, the age model obtained by various methods as above (3.1a–c) suggests that the core top 0 to 85 cm have a sedimentation rate of 4.5 mm/ka, which corresponds to 189 ka. The 85 to 150 cm interval with a sedimentation rate of 2.05 mm/ka covers 320 ka. The highest abundance of Australasian tektite at 170 cm depth suggests a sediment accumulation rate of 0.8 mm/ka and an age between 150 and 200 cm depth covers 649 ka. Based on these sediment accumulation rates, the 2 m-long core bottom may correspond to an age of $\sim$ 1160 ka.

3.2 *Biological productivity*

Among the numerous biological productivity proxies (Ruhlemann *et al* 1999 and references therein), we have used calcium carbonate, organic carbon, total nitrogen and biogenic opal in the present study to trace the biological productivity fluctuations during the past $\sim$ 1100 ka.

3.2a *Calcium carbonate*

Calcium carbonate content of sediment is mainly controlled by the surface water biological productivity, rate of dissolution during its journey through the water column as well as on the seafloor and dilution by the noncarbonate and terrigenous matter. The sediment core under investigation was recovered at a water depth of 5099 m depth, which is well below the carbonate compensation depth (CCD) exhibiting its low carbonate content. Carbonate content has been high (9 wt%) during the last 50 ka and substantially low ($< 1\%$) between 50 ka and 1100 ka (figure 3). The high carbonate content in the last 50 ka could be due to incomplete dissolution of foraminiferal tests as indicated by the presence of a few corroded tests in the coarse fraction. Sediment trap deployed under Environmental Impact Assessment program in the CIOB (10°S: 76°E) at a water depth of 5330 m, and 7 m above the seafloor show 52% calcium carbonate (Parthiban 2000) whereas surface sediments have around 9% carbonate content. This indicates that nearly 85% of carbonate dissolution takes place at the sediment–water interface.

3.2b *Total organic carbon, total nitrogen and C/N ratio*

The factors governing the organic carbon variation are surface water productivity, bottom water oxygen content, degradation, sedimentation rate and bioturbation (Fenney *et al* 1998). The total organic carbon content in the present core varies from 0.1 to 0.6 wt% (figure 3) with an average of 0.2 wt%. This is similar to that of surface sediments earlier estimated from the same basin (Gupta and Jauhari 1994), as well as that of the global average of deep-sea sediments (0.2 wt%) (Degens and Mopper 1976). The low organic carbon content in this area can be attributed to low sediment accumulation rates, which allow more remineralization at the sediment–water interface. The higher water depth (5099 m) at the core site may also facilitate extensive remineralization of organic matter during settling through water column hence, resulting in a low organic carbon content. Sediment trap deployed in the CIOB showed nearly 12% of organic carbon (Parthiban 2000), whereas

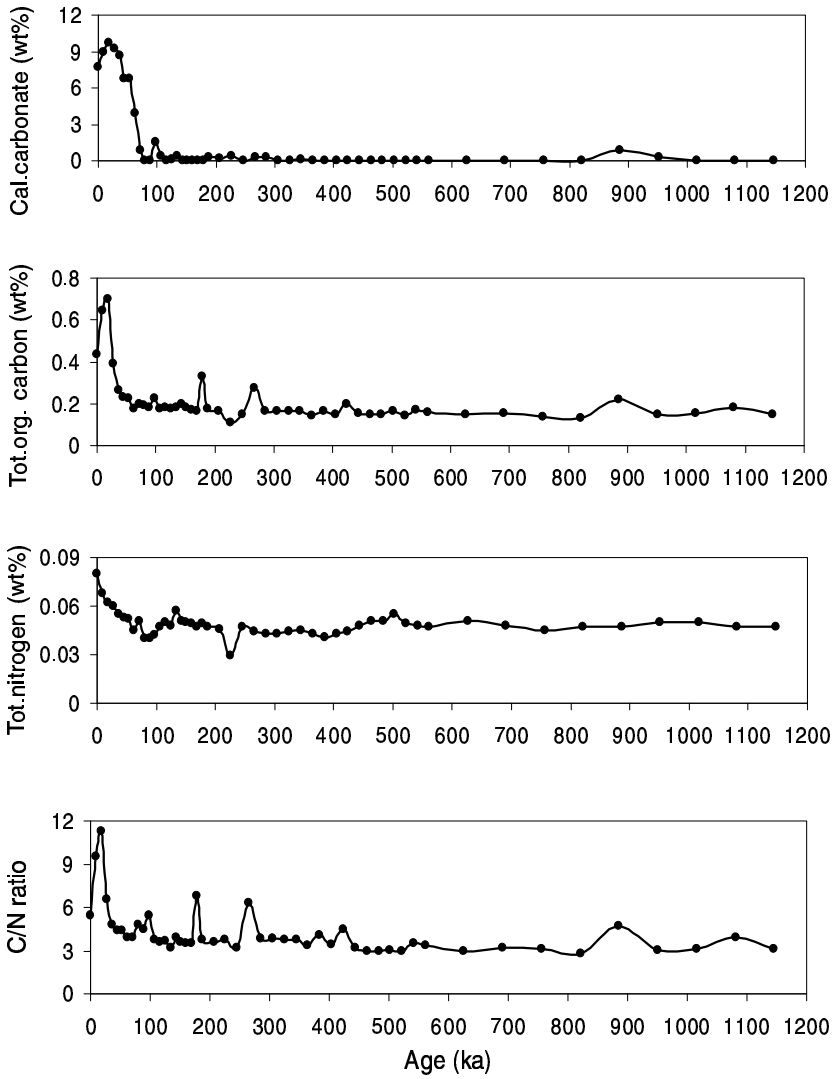

Figure 3. Distribution of calcium carbonate (wt%), total organic carbon (wt%), total nitrogen (wt%) and C/N ratio in a sediment core.

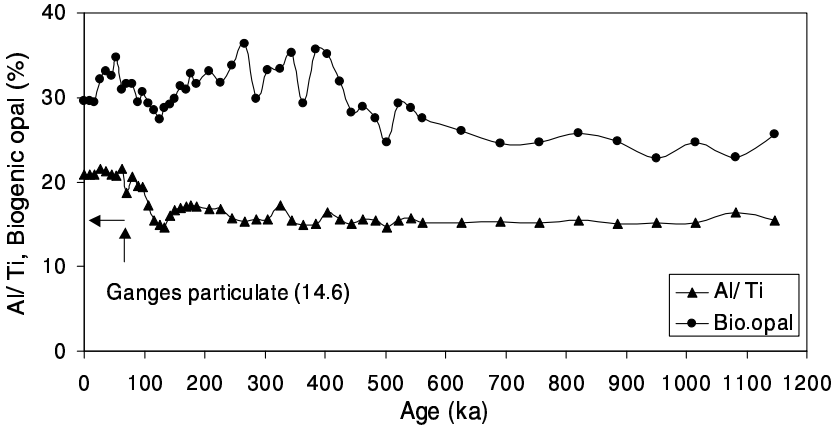

Figure 4. Distribution of biogenic opal (wt%) and Al/Ti ratio in a sediment core. Horizontal arrow indicates Ganges particulate matter Al/Ti ratio.

the average organic carbon content is ~ 0.2 wt% indicating that nearly 60% of organic carbon is degraded at the sediment–water interface. The low organic carbon content in the basin indicates a well-oxidised environment. Such a situation may have been possible due to the influx of Antarctic

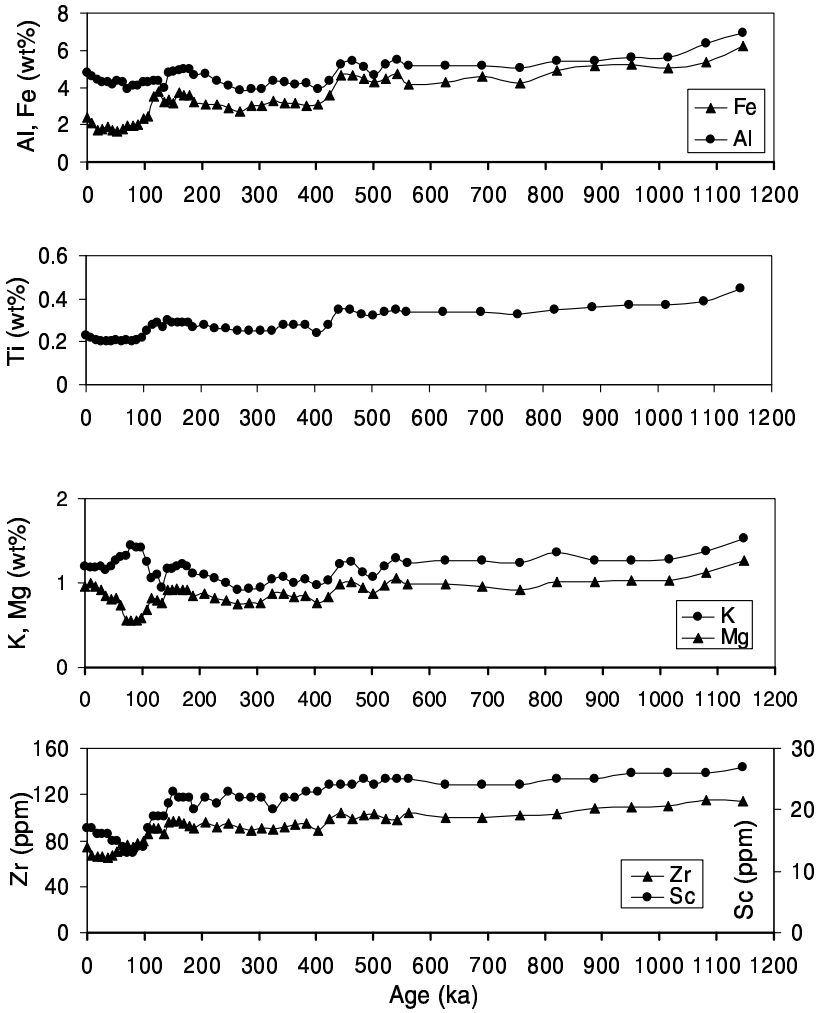

Figure 5. Distribution of Al (wt%), Fe (wt%), Ti (wt%), K (wt%), Mg (wt%), Zr (ppm) and Sc (ppm) in a sediment core.

Bottom Water (AABW) into the basin through the saddle at around 5°S along the Ninety east Ridge (Warren 1982). The AABW, enriched in the dissolved oxygen helps the organic carbon to get oxidized.

The total nitrogen content is very low (< 0.05 wt%), almost constant and follows the total organic carbon distribution pattern (figure 3). The carbon/nitrogen (C/N) ratio in the marine sediments is used to trace the source of organic carbon. For instance, the reported C/N ratio of phytoplankton and zooplankton is ~ 6, for freshly deposited organic matter, this ratio is ~ 10, while terrigenously derived organic matter has this ratio ranging from 20–200 (Meyers 1994; 1997). In the studied sediment core, the C/N ratio is ~ 4 suggesting its marine origin in the past ~ 1100 ka (figure 3). This low C/N ratio could be due to higher inorganic nitrogen (fixed as ammonium ions in the interlayer of clay minerals) and/or better preservation of organic nitrogen compounds by adsorption onto clay minerals (Stevensin and Chen 1972, Muller 1977; Maeda *et al* 2002). Interestingly, in the ODP Leg 116 near the equator (1°S), the organic carbon was found to be of continental origin (France-Lanord and Derry 1997), whereas in sediment core at 13°S the organic carbon is of marine origin. This suggests that terrigenously derived organic carbon has been remineralized within the equatorial zone. Very low and uniform organic carbon content of the sediment core studied here does not allow this to be used as a productivity proxy.

3.2c *Biogenic opal*

Biogenic opal content in the marine sediments has been widely employed as one of the potential paleoproductivity proxy (Charles *et al* 1991). Radiolarians are the prime producers of biogenic opal in the CIOB (Pattan *et al* 1992; Gupta and Jauhari 1994). Biogenic opal in the studied core varies considerably between 21 and 36 wt%. From ~ 400 ka to Present, the content ranges from 25 to 36 wt%

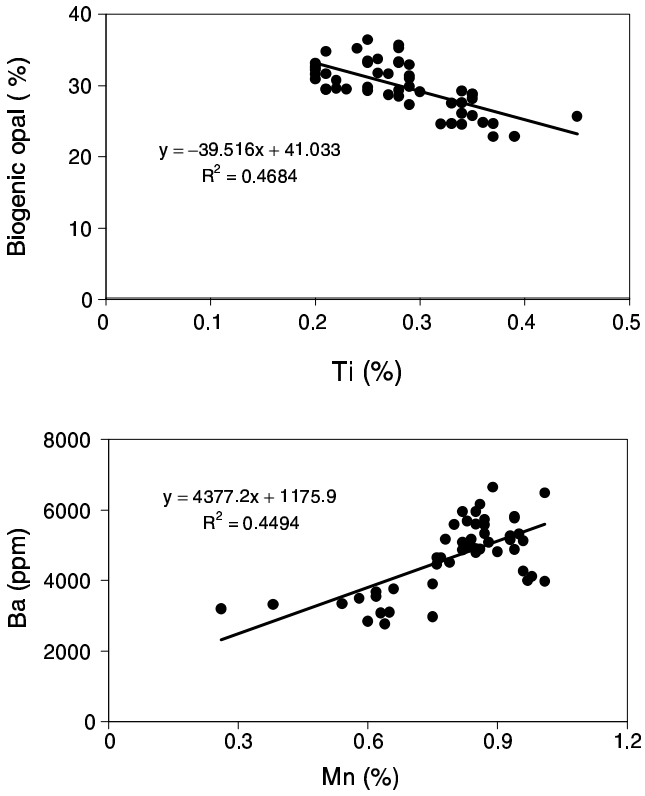

Figure 6. Scatter plot of biogenic opal and Ti content showing inverse relation (top) and Ba and Mn showing a positive correlation (bottom).

with an average of 32 wt% (figure 4). However, from ∼ 400 ka to ∼ 1100 ka, biogenic opal content is comparatively low ranging from 21 to 31 wt% with an average of 26 wt%. This suggests that siliceous productivity was higher (nearly 20%) during ∼ 400 ka to Present compared to the period between ∼ 400 ka and ∼ 1100 ka. This probably suggests the availability of more nutrients resulting in enhanced siliceous productivity. A close look at the biogenic opal distribution during the last ∼ 400 ka shows a concave pattern between 0 and 100 ka, reaching maximum at 50 ka. Further, the pattern shows increasing trend again between ∼ 100 ka and 500 ka (figure 4).

The biogenic opal is the prime carrier of Al excess as shown by the sediment trap samples in the central equatorial Pacific (Dymond *et al* 1997) and the surface sediments of the CIOB (Banakar *et al* 1998) suggesting scavenging of dissolved Al by the biogenic components. Other than biogenic opal, Al excess or Al/Ti ratio could also be contributed by the glass shards of rhyolitic composition (Pattan and Shane 1999) and authigenic clays (Timothy and Calvert 1998). Al/Ti ratio of the sediment varies from 15 to 22 and is highest during the last ∼ 100 ka (20–22). This ratio remains almost constant (15) between ∼ 150 ka and 1100 ka, similar to the Ganges–Brahmaputra particulate matter (figure 4). Though the biogenic opal content is higher during 150 to 400 ka, the corresponding Al/Ti ratio remains as low as that of the Ganges–Brahmaputra matter (15). Whether scavenging by the radiolarians was insufficient or there was an inherent shortage of dissolved aluminum in the water column needs confirmation by further studies.

3.3 *Terrigenous supply*

Strontium and Neodium isotopic studies of sediments from ODP Leg 116 near the equator (1°S) in CIOB suggest that sediments were mostly derived from the metasedimentary rocks of High Himalayan Crystalline (HHC) and a small portion from Lesser Himalayas (LH) and Tibetan Sedimentary Series (TSS) (Bouquillon *et al* 1990; Derry and France-Lanord 1996, 1997). Despite changes in sedimentation rate, tectonics and climate, the source of sediment remained unchanged since ∼ 17 Ma (France-Lanord *et al* 1993). The sediment core under study is located about 1200 km south of ODP Leg 116. The sediments received from the Himalayas near the equator should reach further south in the CIOB by the turbidity currents (Kolla and Biscaye 1973). This is supported from surface sediment geochemistry, flat REE pattern (Nath *et al* 1989; 1992), presence of detrital alumino-silicates in the buried manganese nodules as far as 14°S (Pattan and Banakar 1993) and occurrence of detrital silicate material in a ferromanganese crust (Banakar *et al* 2003). Further, the Wood's triangular diagram of Th, Ta and Hf/3 where all the sediments lie in the field derived from orogenic magma (Pattan, unpublished data), suggests that the detrital material in the CIOB is mainly derived from the Higher Himalayas.

To trace the intensity of Himalayan derived terrigenous material reaching the CIOB, the elements representing detrital origin such as Al, Fe, Ti, K, Mg, Zr and Sc in the sediment core under study were plotted against the age (figure 5). These detrital elements show a strong positive correlation among themselves ($r^2 = \sim 0.8$) suggesting a common source of derivation. The distribution pattern of all these detrital elements suggest that terrigenous input was low during ∼ 400 ka to Present (average: Al – 4.34%, Fe – 2.73% , Ti – 0.25%, Zr – 83 ppm and Sc – 18 ppm) and it increased during ∼ 400 ka and ∼ 1100 ka (average: Al – 5.4%, Fe – 4.7%, Ti – 0.35%, Zr – 103 ppm and Sc – 25 ppm). This indicates that there was nearly 20 to 50% increase of detrital input probably due to the intensification of weathering, erosion of Himalayas and rains which brought the detrital material to the CIOB during ∼ 400 ka to ∼ 1100 ka compared

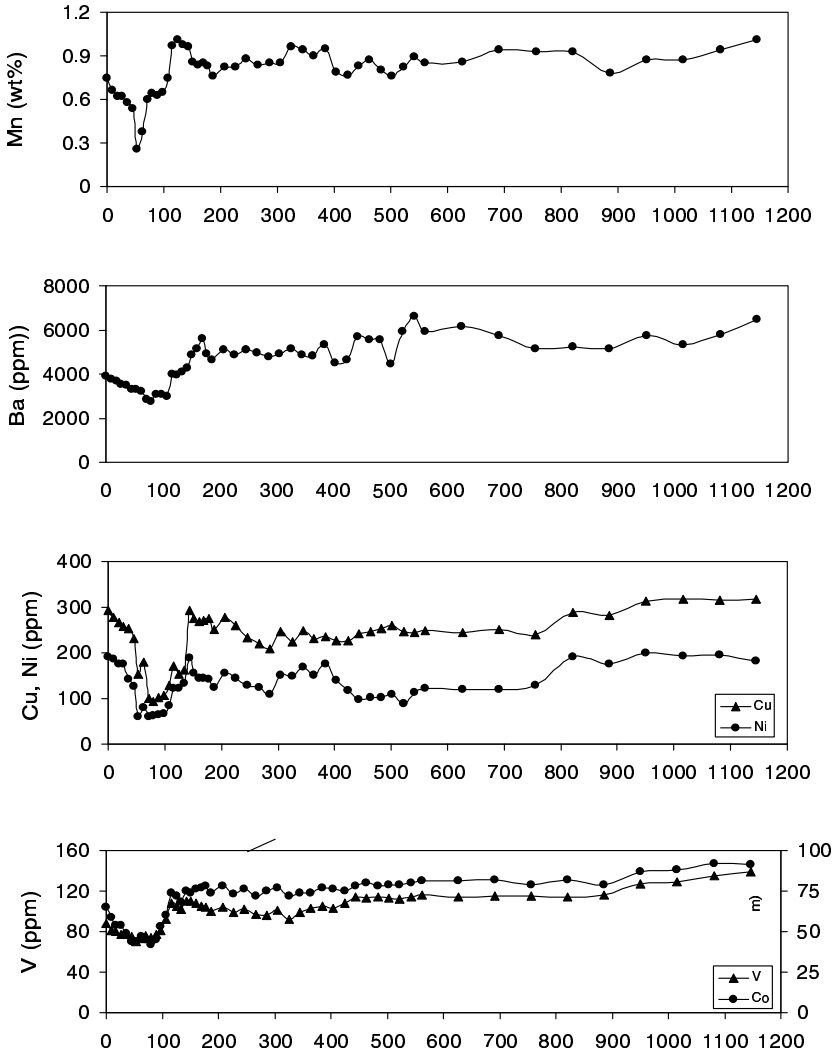

Figure 7. Distribution of bulk Mn, Ba, Cu, Ni, V and Co content in a sediment core.

to the last ~ 400 ka. This finding is further supported by the increased silicate detritus derived from the Himalayas during ~ 700 ka to ~ 2200 ka recorded in Fe–Mn crusts from the same basin (Banakar *et al* 2003). High Himalayan detrital impulse at ~ 500 ka is also reported in a sediment core near the equator (Nath *et al* 2004, in press). Though terrigenous input was low during the last 400 ka, within that period it was lowest from 100 ka to Present which is associated with high biogenic opal. The scatter plot of biogenic opal and Ti (indicative of terrigenous input) shows an inverse relation ($r = 0.69$) suggesting mutual dilution (figure 6). It appears that terrigenous contribution characterized the period between ~ 1100 ka and ~ 400 ka, the later age (400 ka–Present) was marked by increased biogenic contribution. The high and low content of K and Mg at ~ 74 ka is attributed to the presence of Youngest Toba ash, and their distribution pattern almost follows other detrital elements.

3.4 *Noncrustal elements*

Manganese is a redox sensitive element whose concentration is generally high in oxic and low in suboxic or anoxic environments. In the studied sediment core, Mn concentration reached a minimum of 0.3% at ~ 50 ka, suggesting a suboxic or anoxic environment (figure 7). Elements like Cu, Ni, V and Co behave similar to Mn. The distribution pattern of Mn, Ba, Cu, Ni, V and Co remains almost uniform from 150 ka to 1100 ka (figure 7). Manganese, Ba , Ni, Cu, Zn and Co have their excess or noncrustal supply of around 90% of their bulk composition and remained almost uniform during the past ~ 1100 ka (figure 8). This suggests that supply of elemental excess to the seafloor is independent of biogenic or terrigenous input into basin. Ba excess has been used as a paleoproductivity proxy and behaves similar to biogenic opal content (Pattan *et al* 2003 and references therein). In the present sediment core, Ba excess

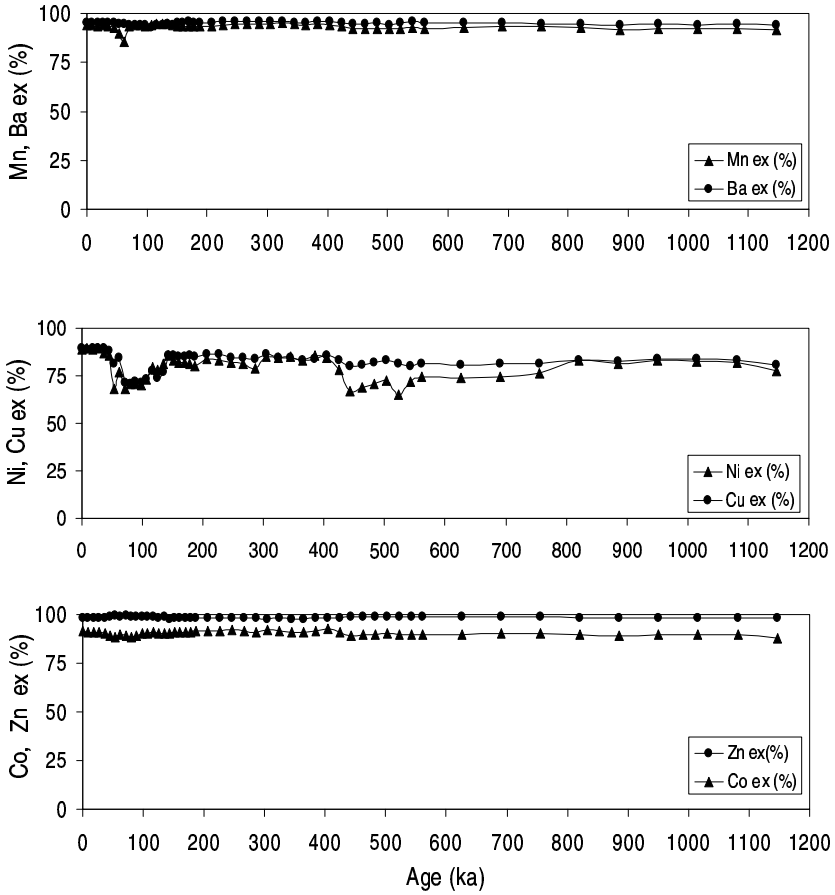

Figure 8. Distribution of elemental excess (Mn, Ba, Ni, Cu, Zn and Co%) in a sediment core.

and biogenic opal do not have any correlation but Ba shows a strong positive correlation with Mn ($r = 0.67$) suggesting removal of Ba through the Mn-oxide phase (figure 9; Banakar *et al* 1998). The Mn oxide phase in the sediment might be in the form of oxide coatings on biogenic components or manganese micronodules. A large number of manganese micronodule abundance is observed in the coarse fraction in these sediments. The observed positive correlation between Ba and Mn could be due to stabilization of todorokite mineral structure in manganese micronodules as a charge balancing cation. Therefore, Ba in the CIOB sediment may not necessarily act as a paleoproductivity proxy always.

4. Conclusions

Based on the records of biological productivity indicators, distribution of terrigenous components and noncrustal/elemental excess in a sediment core from the CIOB during the past $\sim$ 1100 ka, the following conclusions may be drawn.

- In general, the CIOB experienced a fairly well oxidising environment during the past $\sim$ 1100 ka.
- Siliceous productivity was higher during the last $\sim$ 400 ka, whereas detrital material derived from the Himalayas contributed to the bulk of sedimentation during $\sim$ 400 ka to $\sim$ 1100 ka.
- The burial of Mn, Ba, Cu, Ni, Co and Zn excess to the seafloor remained unaffected during the past $\sim$ 1100 ka in spite of variation in siliceous productivity and terrigenous supply.

Acknowledgements

The authors thank the Director, National Institute of Oceanography, Goa for permission to publish. The senior author (JNP) is grateful to the Japan Society for the Promotion of Science (JSPS) for the fellowship. We thank the anonymous reviewers for their constructive suggestions and comments and Dr. S D Iyer and Dr. R Mukhopadhyay for their suggestions and also Dr. M Shyam Prasad for providing the unpublished microtektite data. Thanks are also due to Prof. Basavlingu, Mysore University for the electron microprobe analysis and Dr. V N Kodagali for providing the bathymetric map. This is NIO contribution no. 3938.

References

Aoki S and Sudo T 1973 Mineralogical study of the core samples from the Indian Ocean, with special reference to the vertical distribution of clay minerals; *J. Oceanogr. Soc. Japan* **29** 87–93.

Banakar V K, Gupta S M, Padmavati V K 1991 Abyssal sediment erosion in the Central Indian Basin: Evidence from radiochemical and radiolarian studies; *Mar. Geol.* **96** 167–173.

Banakar V K, Parthiban G, Pattan J N, Jauhari P 1998 Chemistry of surface sediment along a north–south transect across the equator in the Central Indian Basin: An assessment of biogenic and detrital influences on elemental burial on the seafloor; *Chem. Geol.* **147** 217–232.

Banakar V K, Galy A, Sukumaran N P, Parthiban G, Volvaiker A Y 2003 Himalayan sedimentary pulses recorded by silicate detritus within a ferromanganese crust from the Central Indian Ocean; *Earth Planet. Sci. Lett.* **205** 337–348.

Borole D V 1993a Deposition of Mn–Cu–Ni enriched sediments during glacial period in the Central Indian Basin; *Curr. Sci.* **65(10)** 778–782.

Borole D V 1993b Late Pleistocene sedimentation: A case study in the Central Indian Ocean Basin; *Deep Sea. Res.* **40(4)** 761–775.

Bouquillon A, France-Lanord C , Michard A, Tiercelin J J 1990 Sedimentology and isotopic chemistry of the Bengal fan sediments: the denudation of the Himalaya; *Proc. ODP Sci. Results* **116** 43–57.

Brass G W, Raman C V 1990 Clay mineralogy of sediments from the Bengal fan. In: Cochran J R , Stow D A V *et al* (eds) *Proc. ODP Sci. Res.* **116** 35–42.

Charles C D, Froehlich P N, Zibello M A, Mortlock R A, Morely J J 1991 Biogenic opal in southern ocean sediment over the past 450,000 years: Implications for surface water chemistry and circulation; *Paleaoceanography* **6** 697–728.

Caulet J P 1992 Les rapports des campagnes a la mer a bord du Marion-Dufresne, MD65/SHIVA du 17 aout au 14 September 1990. TAAF-MNHN. Paris, p. 53.

Cochran J R 1990 Himalayan uplift, sea level and the record of Bengal fan sedimentation at the ODP Leg site 116 sites. In: Cochran J R, Stow D A V *et al* (eds) *Proc. ODP. Sci. Res.* **116** 397–416.

Debrabant P, Fagel N, Chamley C, Bout V, Caulet J P 1993 Neogene to Quaternary clay mineral fluxes in the central Indian Basin; *Palaeogrogr Palaeoclimat Palaeoecol* **103** 117–131.

Degens E T, Mopper K 1976 Factors controlling the distribution and early diagenesis of organic material in marine sediments. In: Riely J P, Chester R (eds) *Chemical Oceanography*, Pp 60–113.

Derry L A, France-Lanord C 1996 Neogene Himalayan weathering history and river $^{87}Sr/^{86}Sr$: impact on the marine record; *Earth and Planet. Sci.* **142** 59–74.

Derry L A, France-Lanord C 1997 Himalayan weathering and erosion fluxes: climate and tectonic controls. In: Tectonic uplift and climate change, Ruddiman W F (ed.) New York: Plenum press 289–311.

Dymond J, Collier R, McManus J, Honjo S, Manganini S 1997 Can the aluminum and titanium contents of ocean sediments be used to determine the paleoproductivity of the ocean? *Paleoceanography* **12** 586–593.

Fagel N, Debrabant P, Andre L 1994 Clay supplies in the Central Indian Basin since the Late Miocene: climatic or tectonic control? *Mar. Geol.* **122** 151–172.

Fenney B P, Lyle M W, Heath G R 1989 Sedimentation at MANOP site H (eastern equatorial Pacific) over the past 400,000 years: Climatically induces redox variations and their effects on transition metal cycling; *Paleoceanography* **3(2)** 165–189.

France-Lanord C, Derry L A, Michard A 1993 Evolution of the Himalaya since Miocene time: isotopic and sedimentalogical evidence from the Bengal fan. In: Himalayan Tectonics, Treloar P J and Searle M P (eds) *Geological Society of London Special Publication* **74** Pp. 603–621.

France-Lanord C, Derry L A 1997 Organic carbon burial forcing of the carbon cycle from Himalayan erosion; *Nature* **390** 65–67.

Glass B P and Wu J 1993 Coesite and shocked quartz discovered in the Australasian and North American microtektite layers; *Geology* **21** 435–438.

Gupta S M, Jauhari P 1994 Radiolarian abundance and geochemistry of the surface sediments from the central Indian Basin: Inferences to Antarctic bottom water current; *Curr. Sci.* **66(9)** 659–663.

Imai N, Terashima S, Itoh S, Ando A 1995 1994 compilation values for GSJ reference samples. "Igneous rock series"; *Geochim. J.* **29** 91–95.

Kolla V, Biscaye P E 1973 Clay mineralogy and sedimentation in the eastern Indian Ocean; *Deep Sea Res.* **20** 727–738.

Krishnaswami S and Sarin M M 1976 The simultaneous determination of Th, Pu, Ra isotopes ^{210}Pb,^{55}Fe,^{32}Si and ^{14}C in marine suspended phases; *Analytical chimica Acta* **83** 171–181.

Kunzj Bollinger K, Jessberger E K and Storzer D 1995 Ages of Australasian tektites (abstract). Proceedings of the 26th Lunar and Planetary Science Conference. Pp. 809–810.

Maeda L, Kawahata H, Nohara M 2002 Fluctuation of biogenic and abiogenic sedimentation on the Shatsky Rise in the western North Pacific during the late Quaternary; *Mar. Geol.* **189** 197–214.

Meyers P A 1994 Preservation of elemental and isotopic identification of sedimentary organic matter; *Chem. Geol.* **144** 289–302.

Meyers P A 1997 Organic geochemical proxies of paleoceanographic, paleolimnologie and paleoclimatic process; *Org. Geochem.* **29** 213–250.

Mortlock F A, Froelich P N 1989 A simple method for the rapid determination of biogenic opal in pelagic marine sediments; *Deep Sea Res.* **36** 1415–1426.

Mudholkar A V, Pattan J N, Parthiban G 1993 Geochemistry of deep sea sediment cores from the Central Indian Ocean basin; *Ind. J. Mar. Sci.* **22** 241–246.

Muller P J 1977 C/N ratio in Pacific deep sea sediments: Effect of inorganic ammonium and organic nitrogen compounds sorbed by clay; *Geochim Cosmochim Acta* **41** 765–776.

Nath B N, Rao V P, Becker K P 1989 Geochemical evidence of terrigenous influence in deep-sea sediments upto 8°S in the Central Indian Basin; *Mar. Geol.* **87** 301–313.

Nath B N, Roelandts I, Sudhakar M, Pluger W L 1992 Rare earth element patterns of the Central Indian Basin sediments related to their lithology; *Geophy. Res. Lett.* **19** 1197–1200.

Nath B N, Gupta S M, Mislankar P G, Rao B R, Parthiban G, Roelandts I, Patil S K 2004 Evidence of Himalayan erosional event at ~ 0.5 Ma from a sediment core from the equatorial Indian Ocean in the vicinity of ODP Leg 116 sites (in Press, Deep Sea Research Part - II).

Parthiban G 2002 Increased particle fluxes at the INDEX site attributable to simulated benthic disturbance; *Mar. Geores. and Geotech.* **18** 223–235.

Pattan J N, Gupta S M, Mudholkar A V, Parthiban G 1992 Biogenic silica in space and time in sediments of Central Indian Ocean; *Ind. J. Mar. Sci.* **21** 116–120.

Pattan J N, Banakar V K 1993 Rare earth element distribution and behavior in the buried manganese nodules from the Central Indian Basin; *Mar. Geol.* **112** 303–312.

Pattan J N, Shane P, Banakar V K 1999 New occurrence of Youngest Toba Tuff in abyssal sediments of the Central Indian Basin; *Mar. Geol.* **155** 243–248.

Pattan J N, Shane P 1999 Excess aluminum in deep sea sediments of the Central Indian Basin; *Mar. Geol.* **161** 247–255.

Pattan J N, Masuzawa T, Divakar Naidu P, Parthiban G and Yamamoto M 2003 Productivity fluctuations in the southeastern Arabian Sea during the last 140 ka. *Palaeogeog. Palaeoclimat. Palaeoecolog.* **193** 575–590.

Prasad M S and Khedekar V D 2003 Impact microcrater morphology on Australasian microtektites; *Meteoritics and Planetary Science* **38** 1351–1371.

Ruhlemann C, Muller P J, Schneider R R 1999 Organic carbon and carbonate as paleoproductivity proxies: Examples from high and low productivity areas of the tropical Atlantic. In: Use of proxies in Paleoceanography: Examples from the south Atlantic. Fischer G and Wefer G (eds), Berlin Heidelberg: Springler-Verlag, Pp 315–344.

Shane P, Westgate J, Williams M, Korishettar R 1995 New geochemical evidence for the Youngest Toba Tuff in India; *Quat. Res.* **46** 200–204.

Stevenson F J, Chen C N 1972 Organic geochemistry of the Argentine Basin sediments: carbon-nitrogenic compounds sorbed by the clays; *Geochim Cosmochim Acta* **36** 653–671.

Timothy D A and Calvert S E 1998 Systematics of variations in excess Al and Al/Ti in sediments from the central equatorial Pacific. *Paleoceanography* **13(2)** 127–130.

Warren B A 1982 The deep water of the central Indian basin; *J. Mar. Res.* **40** 823–860.

Westgate J A, Shane P A R, Pearce N G J, Perkins W T, Korishettar R, Chesner C A, Williams M A J, Acharyya S K 1998 All Toba tephra occurrences across peninsular India belong to the 75000 yr BP eruption; *Quat. Res.* **50** 107–112.

MS received 12 April 2004; accepted 11 October 2004